



This project has received funding from the European Union's Seventh Programme for research, technological development and demonstration under grant agreement No [308417].



New Directions in Seismic Hazard Assessment through Focused Earth Observation in the Marmara Supersite

Grant Agreement Number: 308417

co-funded by the European Commission within the Seventh Framework Programme

THEME [ENV.2012.6.4-2]

[Long-term monitoring experiment in geologically active regions of Europe prone to natural hazards: the Supersite concept]

D4.6

Report on statistical analysis and modelling of seismic cluster triggering mechanisms

Project Start Date	1 November 2012
Project Duration	42 months
Project Coordinator /Organization	Nurcan Meral Özel / KOERI
Work Package Number	4
Deliverable Name/ Number	Report on statistical analysis and modelling of seismic cluster triggering mechanisms/D 4.6
Due Date Of Deliverable	30/4/2016
Actual Submission Date	30/4/2016
Organization/Author (s)	Hayrullah Karabulut/KOERI Jean Schmittbuhl/ CNRS

Dissemination Level		
PU	Public	
PP	Restricted to other programme participants (including the Commission)	
RE	Restricted to a group specified by the consortium (including the Commission)	
CO	Confidential, only for members of the consortium (including the Commission)	

TABLE OF CONTENTS

<u>1. SEISMIC REPEATERS</u>	<u>3</u>
1.1 DETECTION OF THE SEISMIC REPEATERS	3
1.2 LOCATION ACCURACY OF THE REPEATING EVENTS	4
1.3 SPECTRAL ANALYSIS OF THE REPEATING WAVEFORMS.....	6
<u>2 SEISMIC ACTIVITY RATES</u>	<u>8</u>
2.1 SEISMICITY MAPS OVER THE 2007-2016 PERIOD.....	8
2.2 REGIONAL CUMULATIVE SEISMICITY RATES.....	11

1. SEISMIC REPEATERS

1.1 DETECTION OF THE SEISMIC REPEATERS

Seismicity on creeping sections of the faults produce identical seismograms. These events are named as repeating earthquakes and have been observed at many locations in the creeping sections of the faults. Physical origins of these earthquakes are still being discussed. We searched for seismic repeaters along the Main Marmara Fault (MMF) to detect the possible creeping segments of the fault. The search for the repeaters are performed at several steps. Initially we search earthquakes manually on the continuous recordings of the permanent OBS stations deployed by KOERI and operated between 2011-2013. The main reason to start the search with the OBS station is that they are the closest stations to the fault therefore small magnitude events have better S/N compared to the land stations located at distances > 25km. We then used the manually detected events from the OBSs as templates and perform a more extensive search by cross correlation using the same OBS recordings. This allowed to detect lower magnitude events and possible undetected events. This process was repeated for the 4 OBS sites and we observed several long term repeating earthquakes in the central Marmara basin but none in the Kumburgaz Basin or Cınarcık Basin.

The second step of the search involved the land stations. The origin times of the events detected from the OBS recordings are used to extract waveforms from the recordings of land stations. The waveforms with high S/N are used as templates to detect the events between 2008 and 2015. We used a low threshold for cross correlation coefficient initially to detect low S/N ratio events with less similarity. This allowed to create a large detected waveform database to construct more extensive repeating event waveform catalog. Then we used cross-correlation again to find highly similar events with $CC > 0.9$ from the detected waveform database. Finally the repeaters are selected as waveform with $CC > 0.9$ and with several occurrences from 2008 to 2015.

We also used the waveform database of the events presented in Figure 1 to search for repeaters. We selected stations closest to the fault (SLVM, MARM, MADM, SLVT, TKR, BUY) and waveforms for the events in the existing catalog were cross correlated. After cross correlating between all the pairs of the same station we built an event tree for each station and extract the list of the similar events with $CC > 0.9$. The results were consistent with the results obtained from OBS data. However the number of repeaters detected were greater when we used the OBS data.

An example of the repeaters is presented in Figure 2. The seismic repeaters have been observed from 2008 to 2015 with different recurrence times: from 5 minutes to 9 months. The short term repeaters can be considered as the aftershocks or the foreshocks of the largest events and obey the similar laws as regular earthquakes, e.g., Gutenberg-Richter and Omari law. In Figure 2 we only displayed largest magnitude events during a each occurrence period (few days) of the events. The observation of repeaters is an indication of a continuous

loading of the same rupture zone through time and may be an evidence that the central Marmara region has some creeping behavior at depth.

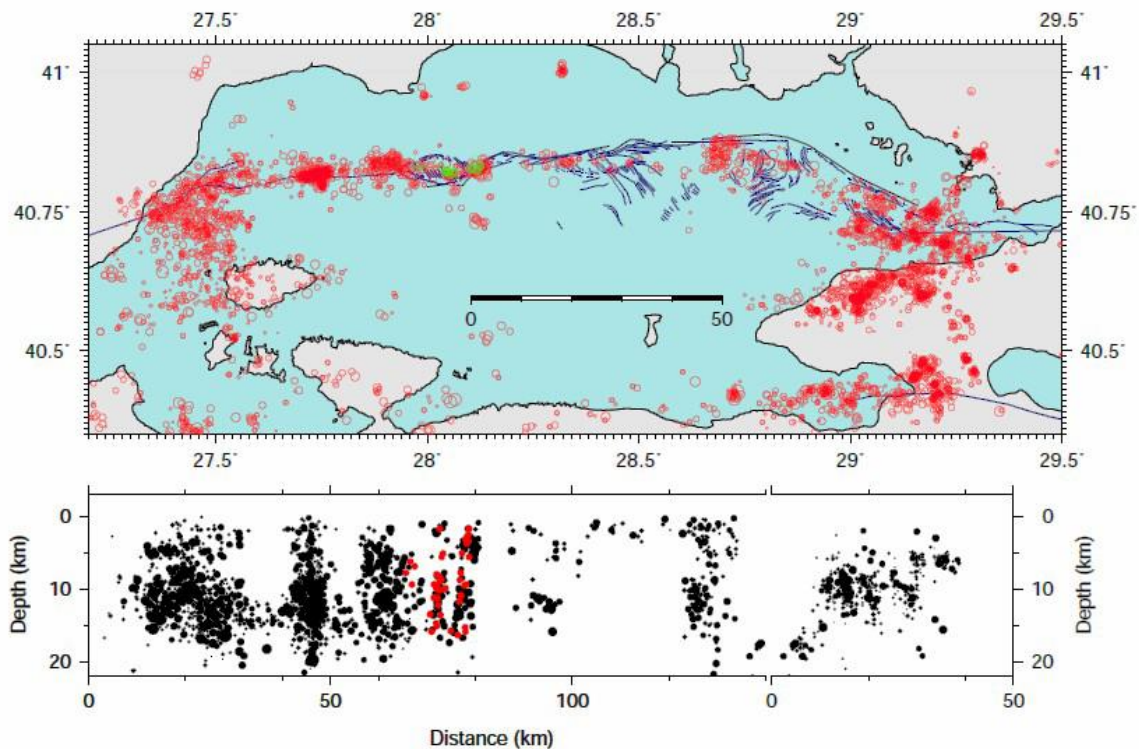


Figure 1: Top : Map view of the seismicity in Marmara region between 2007-2015. The green circles shows the locations of the repeating events. Bottom: Depth view of seismicity. The red circles show the seismic repeaters.

1.2 LOCATION ACCURACY OF THE REPEATING EVENTS

Location accuracy of the repeaters is important to claim that the same asperity is ruptured during each occurrence. To confirm that the events originates from the same or nearly same place, we cross-correlated the events in the cluster shown in Figure 1 with a reference waveform. The reference waveform was chosen as the one with the highest S/N. Figure 3(top) shows the cross correlation values of the traces with reference event. When the CC is high for the S waves and coda delay is small (less than 0.01s) (Figure 3 (middle)). This indicates that the locations of the events are not significantly different within the measurable limits.

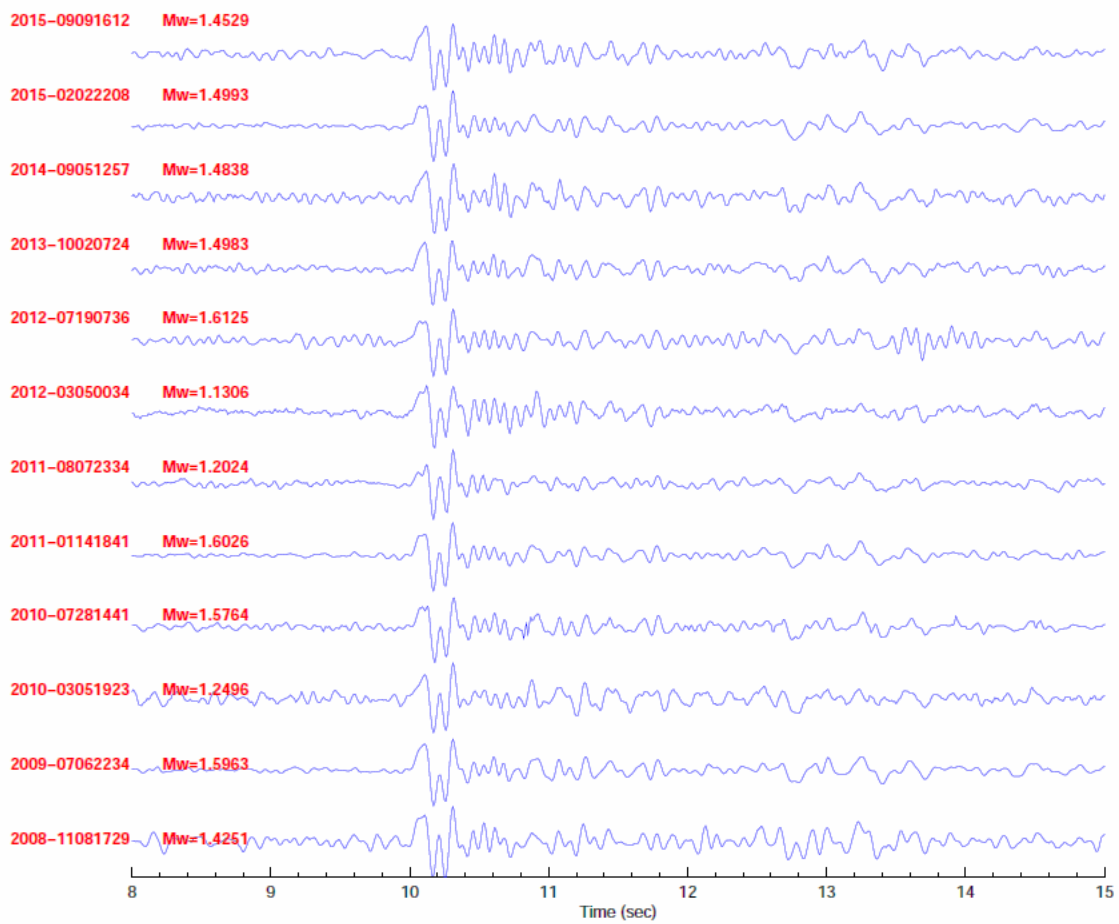


Figure 2: A multiplet detected in the central Marmara. The traces are normalized with the maximum amplitude of the waveform. The origin times of the event is shown on the left with the moment magnitude.

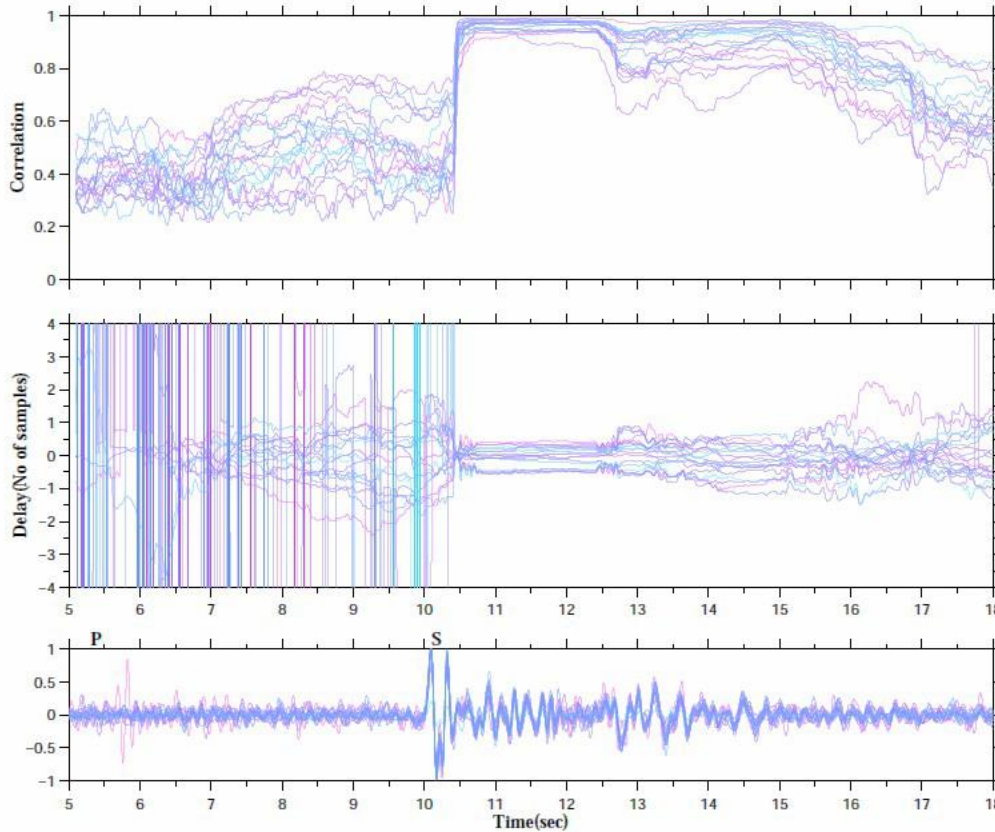


Figure 3: Top: sliding crosscorrelation between waveforms which shows the very small time shift of for S wave and coda: of the order of a few milliseconds (Middle); Bottom: superimposed waveforms after normalization.

1.3 SPECTRAL ANALYSIS OF THE REPEATING WAVEFORMS

We analyzed the waveforms assuming the earthquakes have source regions defined by circular cracks (Brune, 1971). In the classical Brune model, the far-field displacement spectrum $\Omega(\omega)$ of a radiating source has two regions: it is flat at high frequencies, and decays as $\approx \omega^{-2}$, with ω the angular frequency, below the corner frequency f_c . From spectral analysis of the waveforms, the seismic moment M_0 and some source parameters can then be deduced. The mean values for seismic moment M_0 and the corner frequency f_c are obtained from earthquake spectral analysis in the frequency range where the Brune hypothesis is satisfied. We estimate the seismic moment for each waveform and compute the moment magnitude using the equation $M_w = 1.5 \log M_0 - 10.6$ (Kanamori and Anderson 1976) Assuming the representation f_c of a circular source, the radius of the source R , the rupture area A , the maximum slip are estimated following Madriaga (1971). We computed the spectral ratio of the waveforms in each cluster to have a better estimate of the corner frequency. We selected a reference waveform for each cluster as the one with lowest magnitude and S/N greater than 3. When the S/N is high the spectral ratio is flat in the frequency range between 1-15Hz while S/N is low for frequencies > 15 Hz spectral ratio fluctuates. Figure 4(top) shows the spectral ratio of the waveforms displayed in Figure 4(middle). As the magnitudes of the all waveforms are different it is expected that the

corner frequencies will be different. However the relative spectra do not show any differences. Normalized spectral ratios start deviating from their constant value at frequencies greater than 15 Hz. However the influence of intrinsic attenuation is ignored during the analysis and the f_c may be higher.

Figure 4(middle) displays the source parameters of the waveforms shown in Figure 2. We display the magnitudes and slip of each event between 2008 and 2015. Figure 4(bottom) shows the cumulative slip for this repeater and cumulative slip from the tectonic rate with 23 mm/yr.

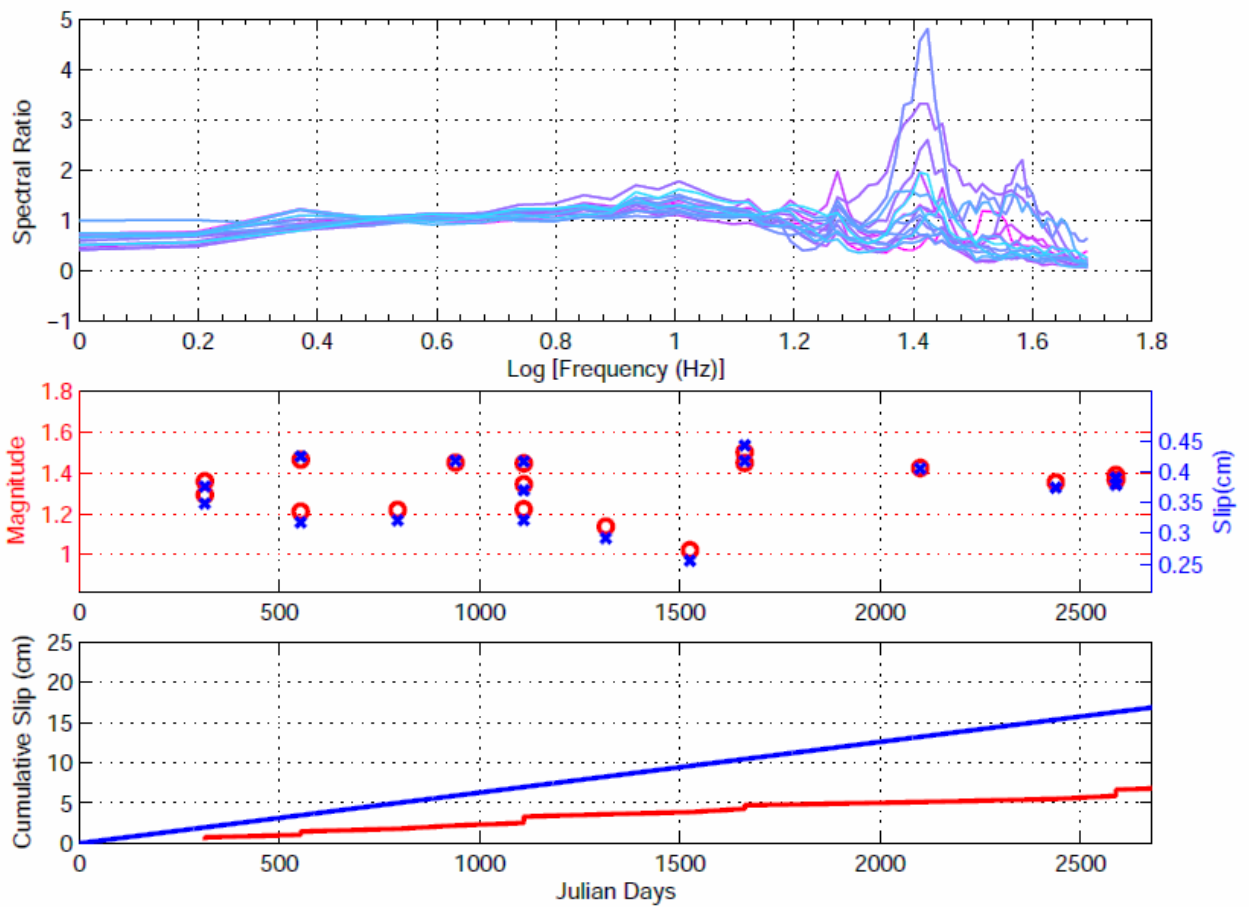
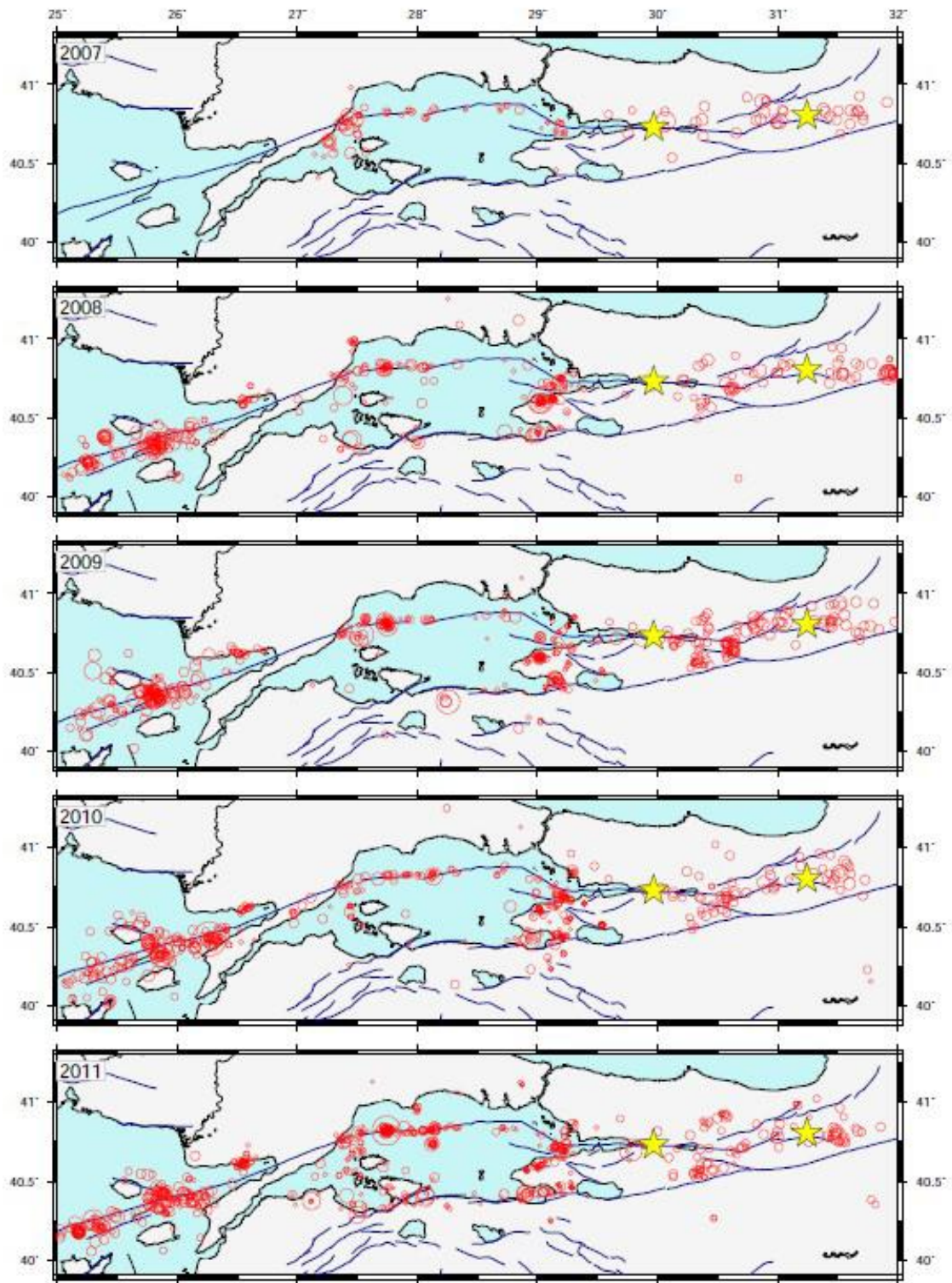


Figure 4: Top : Spectral ratios of the waveforms shown in Figure 1.2. The ratios are approximately flat up to ~ 15 Hz. S/N degrades at frequencies greater than 15 Hz. Middle: Moment magnitudes (red circles) are estimated from the spectra. Slip (blue crosses) for each event is computed assuming a fixed radius estimated from $f_c = 15$ Hz. Bottom: Cumulative displacement of the repeating events from the slips (red) and cumulative displacement from the regional displacement (23 mm/year).

2 SEISMIC ACTIVITY RATES

2.1 SEISMICITY MAPS OVER THE 2007-2016 PERIOD

The temporal and spatial variations of seismicity may indicate some of the deformation in the crust or perturbations in upper mantle structure. It may also be critical to monitor the faults which may be close to the rupture. Furthermore, the geophysical observations have shown that earthquakes can trigger other earthquakes, raising the possibility that earthquake interaction plays an important role in the earth's deformation. We used seismicity catalogs to study the spatial and temporal variations of seismicity in the Marmara region. Figure 5 shows the yearly seismic activities in the Marmara region between 2007-2016. The seismic catalog is more uniform and have a completeness of magnitudes ~ 2.0 after 2009. Both the temporal and spatial distribution of the clusters appear to be quite stable throughout the years. The major change on the seismicity occur during 2014 following the earthquake in Saros.



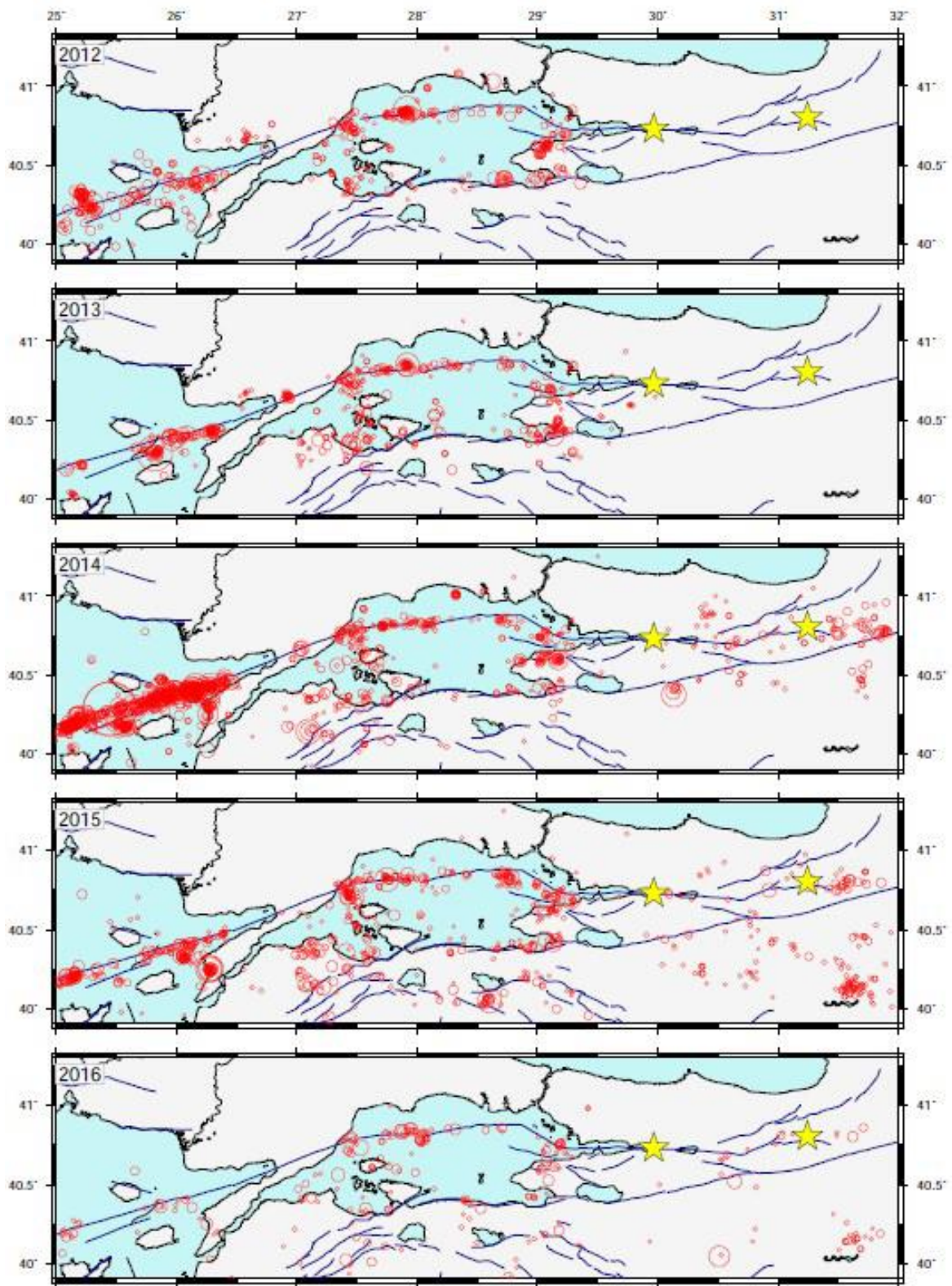


Figure 5: Annual spatial-temporal evolution of the seismicity in the Marmara region between 2007-2016.

2.2 REGIONAL CUMULATIVE SEISMICITY RATES

The cumulative seismicity rates are also good indicators to identify different seismogenic zones. The various sections of the faults may respond to the regional or instantaneous loading in different ways. Figure 6 shows the normalized cumulative seismicity rates for the various sections of the Main Marmara Fault. The rates appear to be significantly different. Two moderate size earthquakes ($M_w=5.2$ and $M_w=4.8$) occurred on the Main Marmara Fault following two moderate size earthquakes ($M_w=6.0$ and $M_w=5.0$) of Simav during 2011 and 2012. The occurrence of these earthquakes also coincides with two large teleseismic earthquakes ($M_w9.0$ Tohoku and $M_w8.6$ Sumatra). Following the 2014 Saros $M_w=6.7$ earthquake, we observe variations on the seismicity rates of the different clusters. This is an indication that the fault segments of the Main Marmara Fault is quite sensitive to the perturbations in the regional stress.

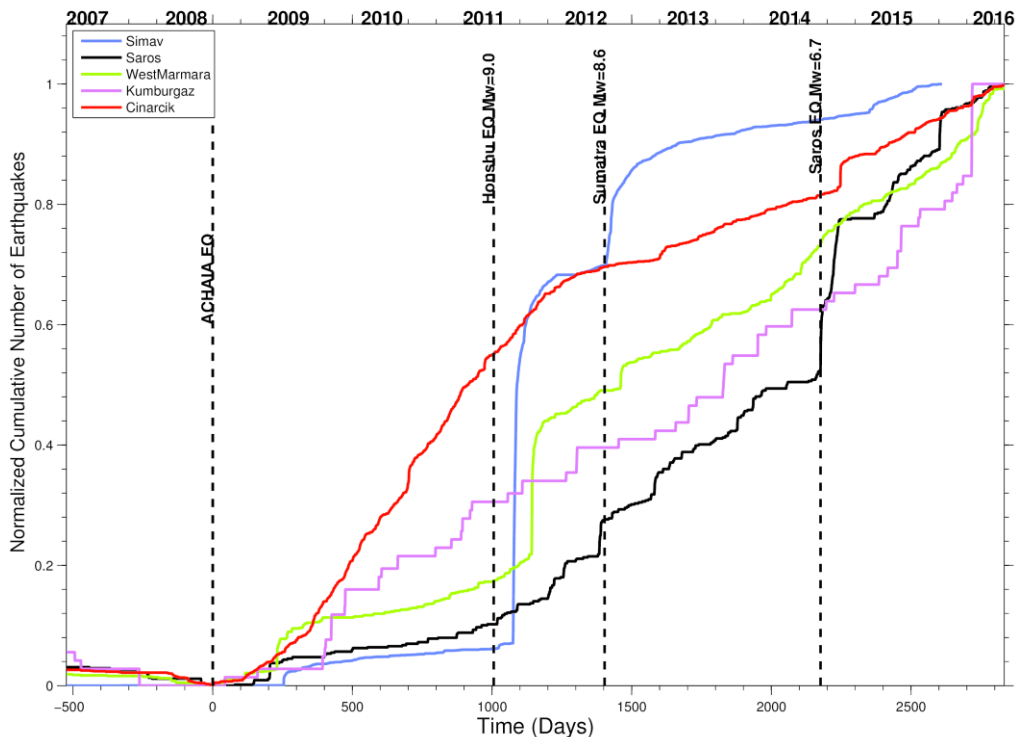


Figure 6: The normalized cumulative seismicity between 2007-2016. The timings of large regional-teleseismic earthquakes are also shown.